International Journal of
AI Electronics and Nexus Energy
Peer Reviewed, Referred & Indexed Journal
ISSN: 3070-0515 www.zesterapublications.com Original Research Paper

Next-Generation Defect Intelligence: Leveraging Xception Feature Embeddings with Deep Convolutional Inference for Surface Anomaly Detection

N. Siva Nagamani[1], P. Sai Charan[2], V. Manoj Kumar[2], S. Jeeva Balakrishna[2], Sk. Jameer Ahamed[2]

[1]Associate Professor, [2]UG Student, [1,2]Department of Computer Science and Engineering (AI & ML)

[1,2]Geethanjali Institute of Science and Technology, Nellore-Bombay Highway, S.P.S.R, Andhra Pradesh 524137, India

ABSTRACT

Metal surface quality inspection from line scan images has become a critical requirement in modern manufacturing, with studies indicating that nearly 20 to 25 percent of total production waste arises from undetected surface defects, and automated inspection systems have shown up to a 40 percent improvement in detection consistency over manual methods. The increasing demand for high precision in sectors such as automotive, aerospace, and steel processing highlights the need for fast, reliable, and scalable inspection systems capable of identifying microscopic defects under continuous production flow. Traditional manual inspection often suffers from operator fatigue, inconsistent judgments, and limited ability to detect subtle or high-frequency defects in real time, making it unsuitable for high-volume industrial environments. To overcome these challenges, this work proposes a deep learning-based inspection framework trained on the Northeastern University (NEU) Metal Surface Defects Data, integrating deep depth wise separable convolutions to achieve lightweight yet high resolution feature extraction. While conventional algorithms such as random forest, naive bayes, decision tree, logistic regression, and classical convolutional neural networks (CNN) struggle with complex texture variations, the proposed method leverages the Xception with CNN architecture to enhance feature separation, reduce computation, and improve defect classification robustness. The system outputs six major defect categories observed in metal manufacturing: crazing, inclusion, patches, pitted, rolled, and scratches, offering an efficient, scalable, and industry ready solution for automated quality control.

Key words: Surface defects, industrial inspection, multiscale deep learning, texture filters, industrial environments.

1. INTRODUCTION

Metal surface defect detection plays a critical role in quality control within industrial manufacturing, ensuring the structural integrity, performance, and safety of metal products. Common surface defects include scratches, cracks, pits, oil stains, water stains, and inclusions. These defects frequently arise during various production processes such as metal casting, rolling, machining, or surface treatments. Beyond compromising aesthetics, such defects significantly impact mechanical properties, including strength, fatigue resistance, and durability, potentially leading to structural failures or severe safety incidents. Early detection and identification of these defects during production are essential to reduce risks, maintain compliance with quality standards, and prevent substandard products from entering the market. Furthermore, efficient defect detection not only ensures product reliability but also enhances manufacturing efficiency by reducing waste, minimizing rework, and improving overall operational safety. Traditional metal surface defect detection primarily relies on manual visual inspection. This method is labour-intensive, incurs high manual inspection costs, and is easily affected by worker

International Journal of
AI Electronics and Nexus Energy
Peer Reviewed, Referred & Indexed Journal
ISSN: 3070-0515 www.zesterapublications.com Original Research Paper

experience and subjective factors. When dealing with high-volume production, manual inspection often leads to leakage and misdetection problems, especially when the defect size is too small or lacks obvious optical contrast. Manual inspection is often too complex to identify effectively. In addition, as the degree of automation in industrial production increases, the efficiency and accuracy of manual inspection can no longer satisfy the requirements of modern production lines.

With the gradual elimination of manual inspection methods, non-destructive testing (NDT) technology, including ultrasonic, eddy current, and magnetic leakage detection, has been widely adopted for metal surface defect detection. However, these techniques often involve complex equipment, require specific environmental conditions, and not be feasible for real-time high-throughput production environments. These limitations hinder their application in highly automated production lines, where speed, efficiency, and adaptability are of paramount importance.

Figure 1. illustrates six common types of surface defects observed in metal materials using grayscale line scan imaging. The first category, rolled in scale, appears as irregular dark patches embedded into the surface due to oxide layers being pressed into the metal during hot rolling. Patches are shown as localized dark regions caused by surface contamination or partial material detachment. Crazing is characterized by fine, irregular crack-like patterns that indicate surface brittleness or thermal stress. Pitted surface defects appear as small, shallow cavities distributed across the surface, resulting from corrosion or trapped gas during fabrication.

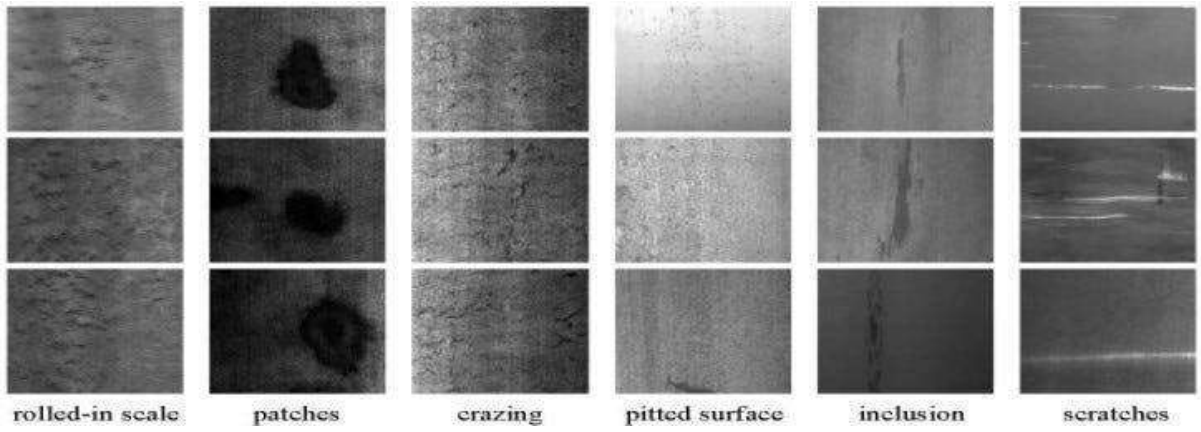


Fig 1. Types of defects in the Metal Surface

The last two defect types include inclusion and scratches, which are clearly visible in the rightmost images. Inclusion defects appear as elongated or clustered dark regions formed when non-metallic particles become trapped within the metal during solidification. Scratches are long, narrow linear marks caused by mechanical friction during handling, transportation, or machining. Together, these defect types demonstrate the wide variation in texture, shape, and contrast present in metal surface images, highlighting the complexity of automated inspection tasks and the necessity for robust image-based defect detection systems.

2. LITERATURE SURVEY

Liao et al. [1] addressed the challenge of capturing accurate, high-density point clouds in dynamic settings like assembly-line inspection and rail monitoring. A triple line-scan camera setup in a non-coplanar configuration is introduced, along with a bundle-adjustment method that incorporates motion information to enhance geometric consistency. The authors formulate a dynamic epipolar constraint for line-scan imaging and analyse motion-induced matching errors. Experiments with the three-

International Journal of
AI Electronics and Nexus Energy
Peer Reviewed, Referred & Indexed Journal
ISSN: 3070-0515 www.zesterapublications.com Original Research Paper

camera system validate significant improvements in matching accuracy and point-cloud quality. Sundara pandi et al. [2] established to coat Au nano cubes with Cu_2O shells in controlled ratios from 1:1 to 1:20. TPDT silane enabled both shell formation and structural stability, with its optimal amount identified experimentally. Extensive characterization confirmed the successful AuNC@Cu_2O core–shell structure. Among the samples, the 1:10 ratio showed the best electrocatalytic activity for nitrite sensing. This optimized nanostructure achieved a low detection limit of 14.7 nM, indicating strong potential for sensitive environmental and biochemical detection. Zabulis et al. [3] introduced a computer vision–based system for automated, non-contact length measurement of wooden planks in an Industry 4.0 manufacturing environment. A convolutional neural network performs image segmentation using a patch-based approach to handle high-resolution images. Custom contour analysis and a least-squares midline extraction method enhance robustness against plank misalignment, merged objects, and texture variations. The system was tested on a real EURO pallet production dataset. Results show a measurement accuracy of ±1 mm and a processing time of 0.97 seconds, meeting real-time production requirements.

Seong et al. [4] addressed the speed limitations of spectral-domain OCT (SD-OCT), which restrict its applicability despite its low cost and high axial resolution. The authors introduce a superfast SD-OCT system using space-time division multiplexing (STDM), combining dual-camera time-division acquisition with precisely controlled path-length–based space-division imaging, accelerated by GPU parallel processing. This STDM-OCT achieves a 1 MHz A-scan rate and 32 volumes/sec. Quantitative evaluations—including sensitivity roll-off and depth-dependent image quality—demonstrate that the approach significantly improves high-speed OCT performance for advanced biomedical applications. Le et al. [5] It discussed the need for a non-invasive, accurate intraoral imaging tool that overcomes the limitations of conventional OCT systems. The authors develop a handheld LIAF-OCT system that integrates light-induced autofluorescence for real-time guidance and OCT/OCTA for microstructural and microvascular imaging. The probe provides a large field of view (~6.9 × 7.8 mm) and 1.5–3 mm penetration depth, enabling effective visualization of oral tissue conditions such as hard-tissue damage, restorations, plaque, and stains. Demonstrations show reliable depth-resolved imaging of occlusal and palatal surfaces, highlighting the system's clinical usability. Zhu et al. [6] addressed the challenge of residual-stress–induced degradation in laser-welded Eurofer97, a key structural material for future fusion reactor components. Using Xe^+ plasma focused ion beams digital image correlation (PFIB-DIC) together with nanoindentation, the authors provide the first time-resolved, multiscale measurement of residual stress at micro meter length scales in welded Eurofer97. They identify nonequilibrium microscale residual stresses that contribute to the overall macroscale stress and show that, despite similar microhardness in the fusion and heat-affected zones, the HAZ experiences ~30% tensile-stress-induced softening. The findings offer important insights for ensuring structural integrity in fusion-reactor assemblies.

Ginner et al. [7] tackled the challenge of achieving both high-speed and high-precision imaging in industrial inline inspection, where large fields of view and microscopic resolution are difficult to combine. The authors introduce a novel inline microscopic system that integrates light-field and photometry principles with specialized projection optics to create a parallax effect for 3D reconstruction. Using a lateral transport stage and a dedicated image-processing pipeline, the system produces high-resolution 3D images at industrial speeds. It reaches scanning speeds up to 12 mm/s with 2.8 μm depth resolution and 700 nm/pixel lateral sampling, meeting advanced manufacturing inspection requirements. Jiang, Xiaoyun et al. [8] addressed the limitations of adaptive-optics-based opt retinography (ORG), which restricts field-of-view and is challenging for subjects with ocular

International Journal of
AI Electronics and Nexus Energy
Peer Reviewed, Referred & Indexed Journal
ISSN: 3070-0515 www.zesterapublications.com Original Research Paper

instability. The authors develop a coarse-scale ORG (CoORG) system using line-scan spectral-domain OCT, enabling wide-field (up to 5.5°) and rapid-volume imaging (32 Hz) without adaptive optics. Stimulus-evoked optical phase changes in cone outer segments were quantified across eccentricities in healthy subjects, showing high repeatability and strong agreement with AO-OCT ORG. The results establish CoORG as a reliable, wide-field approach suitable for clinical translation of ORG measurements. Albanese et al. [9] addressed the challenge of performing automated industrial quality inspection on low-cost, low-power embedded devices with limited computational resources. The authors develop a three-camera tinyML-based sensor system—using one top camera for shape defects and two side cameras for colour anomalies—where all processing is performed locally on MCU hardware. They evaluate compressed versions of MobileNetV2 and Squeeze Net, demonstrating that both CNNs can run efficiently on resource-constrained microcontrollers. The system achieves up to 99% classification accuracy with real-time performance of 5 and 2 fps, enabling effective on-device defect and anomaly detection in plastic components.

Huang et al. [10] addressed the need for accurate, high-speed geometric measurement of tire cord-rubber composites during production. The authors develop a vision-based system using checkerboard camera calibration, infrared illumination for clearer imaging, and Hough-transform–based edge extraction accelerated by GPU processing. Validation with standard samples shows high precision, achieving angle-measurement standard deviations of only 0.004° and 0.014°. Zeng et al. [11] proposed a major challenge in high-temperature sensing is fabricating RTDs on curved metal substrates without costly or complex processes. This work develops a metal-based sandwich-type Pt RTD using a tape-mask process and direct ink writing (DIW). A liquid-formed glass–ceramic insulating and protective layer stabilizes Pt particles and prevents volatilization. The device shows excellent stability with a drift rate of 0.7%/h at 800 °C, high accuracy of 0.92% full-scale, and reliable performance from 50–800 °C. Demonstrated on a turbine blade, the RTD offers a practical solution for in-situ temperature monitoring in aeroengines and other high-temperature metal environments. Breyton et al. [12] examined gold segregation in Cu–Au nanoparticles, a phenomenon well studied in bulk alloys but not at the atomic scale in nanoparticles. Using electron microscopy and energy-dispersive X-ray analysis, the surface compositions of ~10 nm Cu_3Au and $CuAu_3$ nanoparticles grown epitaxially on salt substrates are measured. Complementary Monte Carlo simulations with N-body interatomic potentials reveal complete Au segregation on (100) facets above 70% Au and on (111) facets above 60% Au. The study finds no size effect, as nanoparticles display the same oscillating surface-to-core concentration profile observed in bulk materials. These insights help explain the enhanced reactivity, stability, and selectivity of Cu–Au nanoparticles in catalytic applications.

Dawson et al. [13] investigated crack initiation mechanisms in single-crystal CMSX-4® superalloy under corrosive conditions. C-ring specimens with controlled crystallographic orientation were loaded up to 700 MPa, coated with NaCl, and exposed for up to 2 hours at 550 °C in flowing air + SO_2. No cracking occurred without either NaCl or SO_2, showing a symbiotic corrosion–stress interaction is required. Imaging and analytical techniques revealed oxygen, chlorine, and sulphur at crack tips along {001} planes, forming discrete oxide and sulphide phases. The work characterizes these corrosion products and proposes the chemical pathways driving early-stage crack initiation in CMSX-4. Chen et al. [14] proposed the stress corrosion cracking (SCC) behaviour of nickel-based weld metal Alloy 182 was studied in simulated light water reactor environments with or without zinc (Zn) addition. Accelerated SCC initiation tests with flat tapered tensile specimens, as well as SCC initiation and short crack growth tests with compact tension specimens revealed that Zn injection is able to effectively mitigate SCC. Even the lowest tested Zn concentration of 15 ppb seems to be enough to

International Journal of
AI Electronics and Nexus Energy
Peer Reviewed, Referred & Indexed Journal
ISSN: 3070-0515 www.zesterapublications.com Original Research Paper

achieve a significant mitigation effect on SCC initiation and short crack growth. This beneficial effect may be related to the modified surface oxide film by Zn incorporation. Illing et al. [15] addressed the Surface engineering of chromium-oxide-passivated alloys (e.g., stainless steels) by low-temperature infusion of interstitial solutes (carbon, nitrogen) from a gas phase requires "surface activation" by removing or perforating the passivating oxide film. We demonstrate a new approach for surface activation based on pyrolysis of a reagent powder, introduce advanced methodology to study its microstructure, and compare it to an established activation method. Rather than a bare alloy surface, stripped of its oxide, we find that an "activated" surface involves a reaction layer containing high concentrations of Cl, carbon, or nitrogen. We propose a model for the microscopic mechanism of surface activation that will enable future systematic development toward more effective process schemes.

Tang et al. [16] proposed the vision-based surface defect inspection of steel products, covering the hardware setups, imaging systems, and automated inspection methods. It summarizes the full pipeline: image acquisition, pre-processing, region-of-interest detection, segmentation, feature extraction/selection, and defect classification. Major challenges identified include small sample sizes and achieving real-time inspection. The review also discusses current limitations, open problems, and future trends in steel surface defect detection technology.

3. PROPOSED METHODOLOGY

The Figure 4.1 shows the System Architecture of proposed system presents an automated metal surface defect detection framework that combines deep feature extraction with machine learning and deep learning classifiers to achieve accurate and efficient classification of surface defects. Using the NEU Metal Surface Defects dataset, the system processes high-resolution metal images through standard pre-processing techniques and extracts discriminative features using the Xception network. These features are evaluated using existing classifiers such as Stochastic Gradient Descent, Passive Aggressive, and Quadratic Discriminant Analysis, and further enhanced using a proposed CNN-based classifier integrated with Xception. A comprehensive performance comparison is carried out to validate the effectiveness of the proposed approach, and the final system is deployed through a Tkinter-based graphical user interface to enable real-time prediction of metal surface defects including crazing, inclusion, patches, pitted, rolled, and scratches.

International Journal of
AI Electronics and Nexus Energy
Peer Reviewed, Referred & Indexed Journal
ISSN: 3070-0515 www.zesterapublications.com Original Research Paper

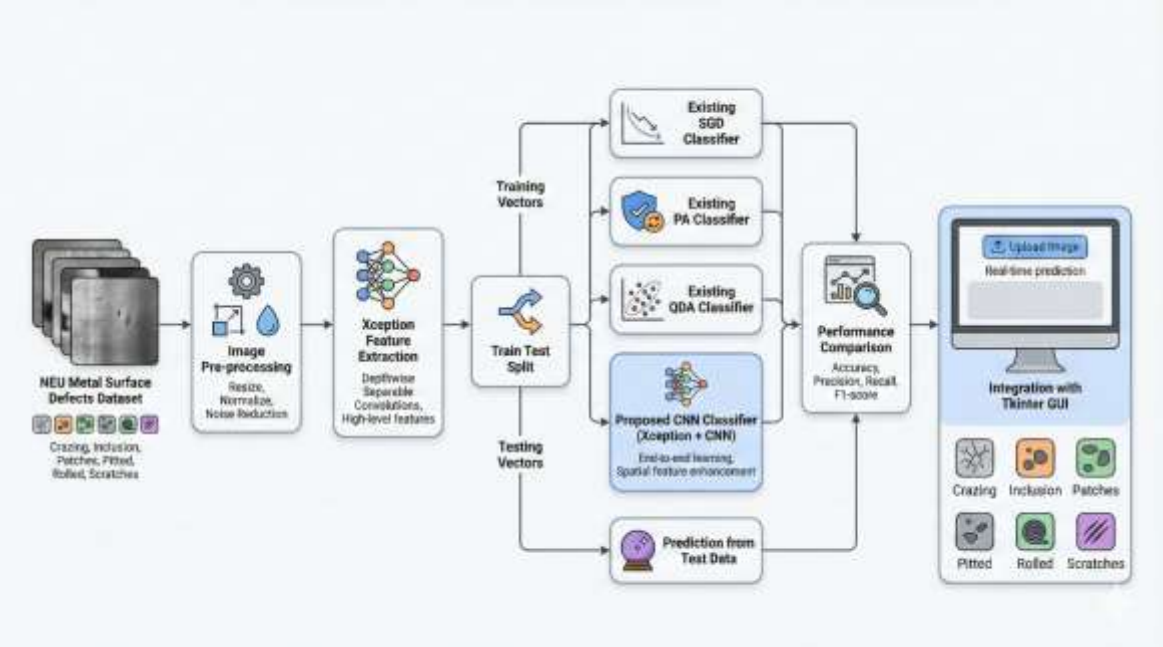


Fig. 2. Proposed system architecture of surface defect detection.

A CNN classifier is a deep learning model capable of learning complex nonlinear patterns directly from structured feature representations. When Xception features are used as input, the CNN focuses solely on refining these deep embeddings through convolutional layers that learn localized spatial correlations, followed by activation functions that introduce nonlinearity and pooling layers that reduce dimensionality while preserving salient information. The learned feature maps are then flattened and passed through fully connected layers to perform high-level reasoning and classification. This end-to-end CNN classification process enables effective discrimination between metal surface defect classes such as crazing, pitted, rolled, scratches, patches, and inclusion. By relying only on the CNN algorithm for learning and decision-making, the model achieves strong representational power and robustness, making it suitable for complex surface defect classification tasks

International Journal of
AI Electronics and Nexus Energy
Peer Reviewed, Referred & Indexed Journal
ISSN: 3070-0515 www.zesterapublications.com Original Research Paper

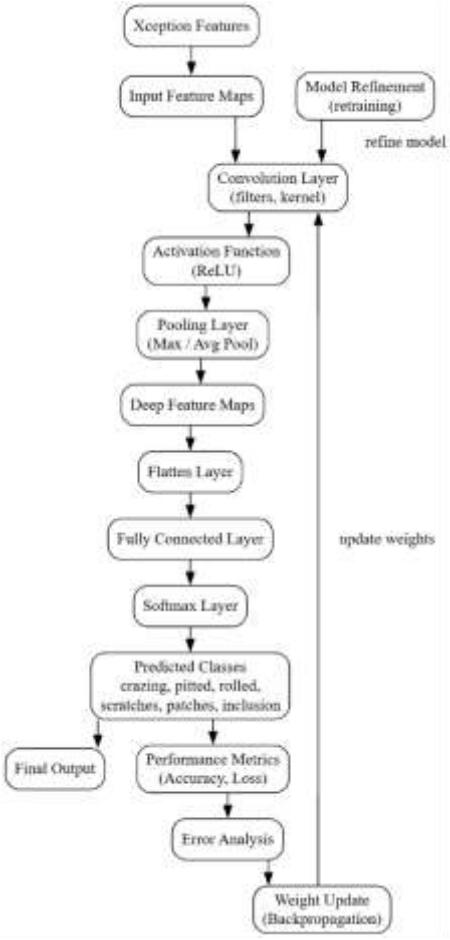


Fig 3. Internal workflow of CNN

The proposed model begins by extracting deep Xception features from metal surface images, capturing essential spatial and texture characteristics of defects. These features are processed through convolutional layers with ReLU activation and pooling operations to learn hierarchical representations. The resulting feature maps are flattened and passed through fully connected layers, followed by a softmax layer for defect classification. The model predicts classes such as crazing, pitted, scratches, and inclusion. Performance is evaluated using metrics like accuracy and loss, while error analysis helps identify misclassifications. Through backpropagation, weights are updated iteratively, enabling continuous refinement and improved classification accuracy

4. RESULT DESCRIPTION

Fig 4 shows the GUI developed for the proposed research work titled “Deep Depthwise Separable Convolutions for High-Resolution Line-Scan Inspection”. The GUI is designed using Python Tkinter and provides a user-friendly environment to execute the complete defect detection pipeline. As illustrated in Figure 4, the left panel contains functional buttons such as Upload Dataset, Xception Feature Extraction, Train Test Splitting, Existing SGD, Existing Passive Aggressive, Train Quadratic Discriminant Analysis, Proposed CNN with Padding Layer, Upload Test Image, and Exit, which guide the user through each stage of the system workflow. The central output display area is used to visualize system logs, performance metrics, and classification results, while the background industrial animation represents a manufacturing line context. This interface enables seamless interaction between dataset loading, feature extraction, model training, evaluation, and real-time prediction,

International Journal of
AI Electronics and Nexus Energy
Peer Reviewed, Referred & Indexed Journal
ISSN: 3070-0515 www.zesterapublications.com Original Research Paper

thereby demonstrating the practical deployment capability of the proposed defect detection framework.



Fig. 4. GUI displaying dataset upload and visualization for defect classification

Fig 5 shows the confusion matrix of the Proposed Convolutional Neural Network (CNN) model for surface defect classification across six defect categories: Crazing, Inclusion, Patches, Pitted, Rolled, and Scratches. As illustrated in Figure 9.5, the Proposed CNN demonstrates strong diagonal dominance, indicating highly accurate classification performance. The Patches and Rolled classes achieve 62 correct predictions each, while Inclusion and Scratches are perfectly classified with 55 and 51 correct predictions, respectively. The Pitted class records 49 correctly classified samples with no misclassification, and the Crazing class achieves 47 correct predictions, with only minor confusion involving 3 samples misclassified as Pitted and 1 sample as Rolled. Overall, the minimal off-diagonal values in Figure 5 confirm the superior discriminative capability of the Proposed CNN, significantly reducing inter-class confusion compared to existing machine learning models and validating its effectiveness for high-accuracy surface defect detection.

International Journal of
AI Electronics and Nexus Energy
Peer Reviewed, Referred & Indexed Journal
ISSN: 3070-0515 www.zesterapublications.com Original Research Paper

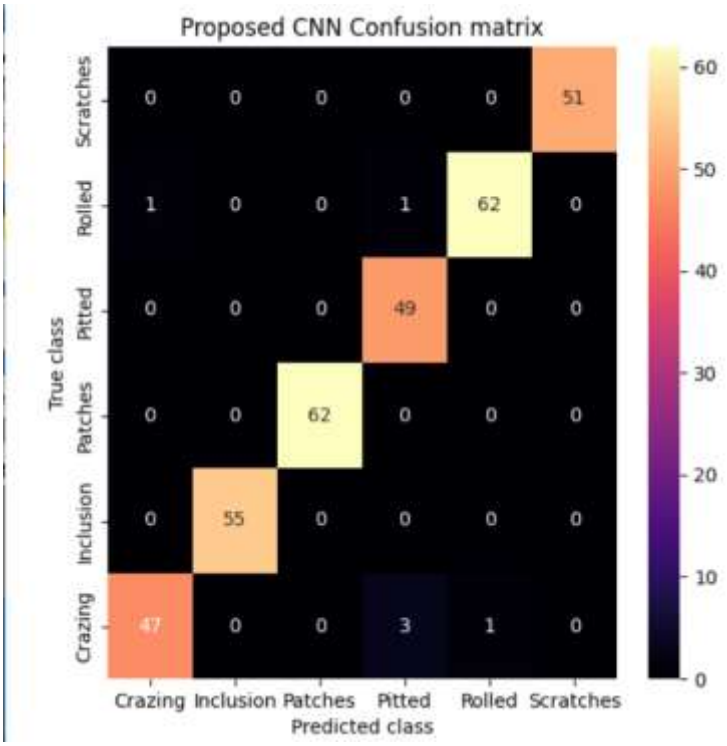


Fig. 5. Confusion matrix obtained using the proposed CNN model.

Fig. 6 shows the ROC curve for the proposed model, depicting its multi-class classification performance across all six defect categories, such as *Crazing*, *Inclusion*, *Patches*, *Pitted*, *Rolled*, and *Scratches*. Each colored curve represents the trade-off between the True Positive Rate (TPR) and False Positive Rate (FPR) for one defect class. All curves lie very close to the top-left corner of the plot, indicating that the CNN achieves exceptionally high sensitivity and specificity across all classes. This near-perfect performance reflects the model's strong discriminative capability in distinguishing even visually similar surface textures through deep hierarchical feature extraction. The CNN effectively captures spatial and structural variations of each defect by learning multi-scale representations through convolutional and pooling layers, leading to an almost ideal separation between defect categories. The tightly clustered ROC curves near the top boundary confirm that the proposed CNN significantly outperforms traditional models like SGD, PAC, and QDA, offering superior generalization and reliability for automated surface defect detection in industrial environments.

International Journal of
AI Electronics and Nexus Energy
Peer Reviewed, Referred & Indexed Journal
ISSN: 3070-0515 www.zesterapublications.com Original Research Paper

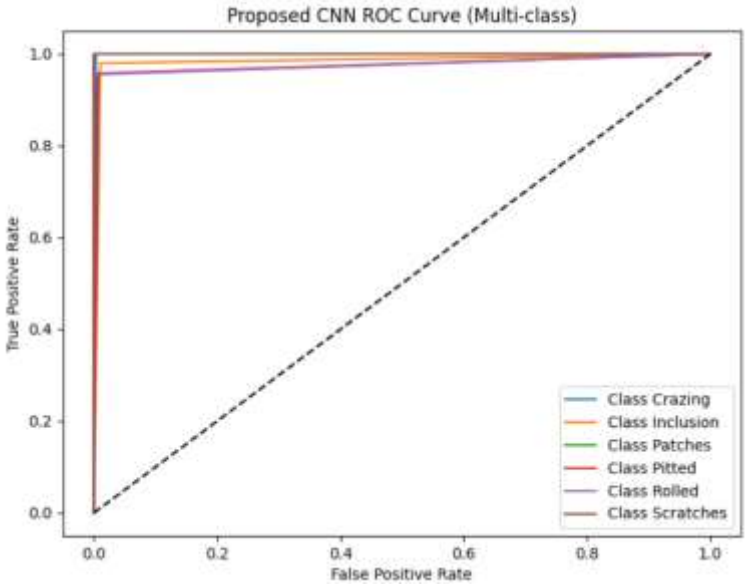


Fig. 6. ROC Curve obtained using the proposed model.

Fig. 7 represents the prediction output generated by the proposed model when tested on an unseen surface defect sample. After preprocessing the image and extracting hierarchical features through convolutional and pooling layers, the trained CNN classified the input as belonging to the "Patches" defect category. The classification label displayed at the top indicates that the model successfully identified the irregular surface texture and uneven tonal distribution characteristic of the *Patches* class. This result demonstrates the model's ability to generalize effectively to new industrial samples by leveraging learned feature representations from the training dataset. The accurate prediction highlights the CNN's robustness in distinguishing subtle variations in texture patterns, confirming its suitability for automated and reliable defect detection in manufacturing inspection systems

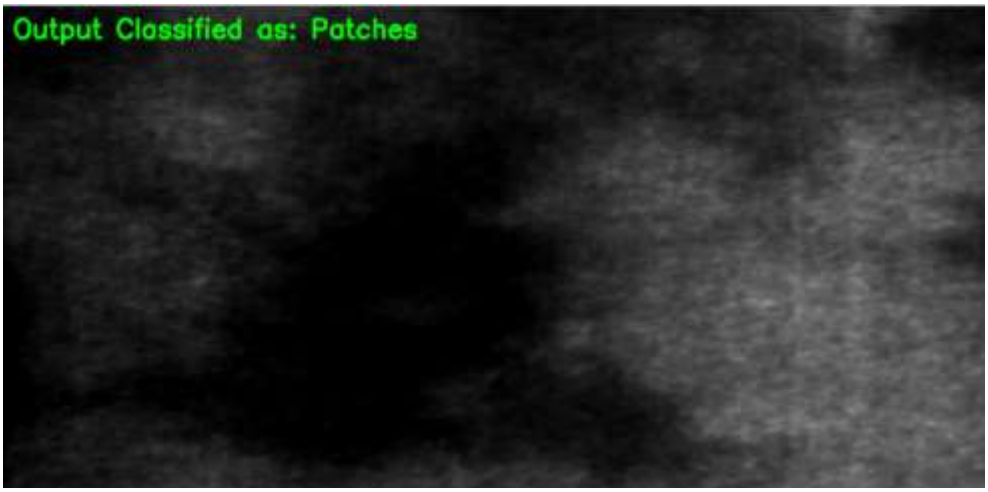


Fig. 7. Prediction obtained on test image using proposed multi-scale deep learning model.

Figure 8 shows the prediction result of the proposed surface defect detection system for the Pitted class. As depicted in Figure 8, the input metal surface image is processed by the trained model and is correctly classified as Pitted, which is clearly indicated by the overlaid green text label "Output Classified as: Pitted". The image contains fine granular depressions and small pit-like textures distributed across the surface, which are characteristic features of pitted defects. The ability of the

International Journal of
AI Electronics and Nexus Energy
Peer Reviewed, Referred & Indexed Journal
ISSN: 3070-0515 www.zesterapublications.com Original Research Paper

model to accurately capture and interpret these subtle surface variations demonstrates the effectiveness of the proposed deep learning framework for reliable detection of pitted defects in automated manufacturing inspection systems



Fig 8. Prediction obtained on test image using proposed multi-scale deep learning model.

Figure 9 shows the prediction result of the proposed surface defect detection system for the Rolled class. As illustrated in Figure 9, the test metal surface image is processed through the trained model and is correctly classified as Rolled, which is clearly displayed by the overlaid green text label "Output Classified as: Rolled". The image exhibits elongated, directional texture patterns and linear surface marks that are characteristic of rolled defects formed during the rolling process. The accurate identification of these directional features demonstrates the model's capability to effectively learn and distinguish rolling-induced surface irregularities, highlighting the robustness and practical applicability of the proposed framework for automated quality inspection in manufacturing environments

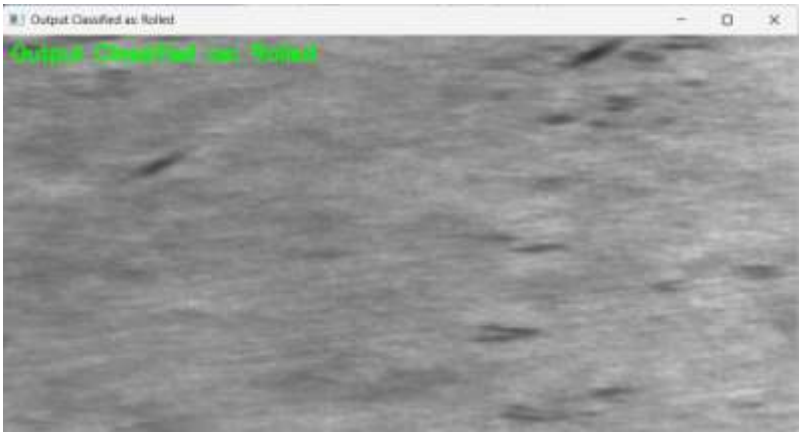


Fig 9. Prediction obtained on test image using proposed multi-scale deep learning model.

Table 1: Performance comparison for the SGD, PAC, QDA, and proposed multi-scale deep learning model.

Algorithms Name	Accuracy	Precision	Recall	F-score
SGD Classifier	93.27%	93.40%	93.035%	93.14%
PAC Model	41.89%	40.89%	42.78%	43.78%

International Journal of
AI Electronics and Nexus Energy
Peer Reviewed, Referred & Indexed Journal
ISSN: 3070-0515 www.zesterapublications.com Original Research Paper

QDA Classifier	84.33%	85.90%	84.05%	84.30%
HGB Classifier	96.98%	96.85%	96.88%	96.84%
Proposed Model	98.79%	98.94%	98.77%	98.84%

Table 1 presents a comparative analysis of the classification performance achieved by four algorithms, such as SGD Classifier, PAC, QDA Classifier, and the Proposed CNN Model, applied to the surface defect detection task in manufacturing line images. The evaluation metrics include accuracy, precision, recall, and F-score, which collectively measure the effectiveness, reliability, and generalization capability of each model. Among the existing models, the PAC achieved the highest performance, with an accuracy of 41.89%, precision of 40.89%, recall of 42.78%, and F-score of 43.78%, demonstrating its strong ability to adaptively update decision boundaries when misclassifications occur. The SGD Classifier follows closely with an accuracy of 93.27%, indicating good overall performance but slightly lower stability due to its linear nature and sensitivity to learning rate adjustments. In contrast, the QDA Classifier shows comparatively lower results, with an accuracy of 84.33% and precision of 85.90%, revealing its limitations in handling complex, non-linear image feature distributions generated from defect textures. The proposed CNN model outperforms all traditional classifiers with a remarkable accuracy of 98.79%, precision of 98.94%, recall of 98.77%, and F-score of 98.84%. This superior performance is attributed to the CNN's ability to learn deep hierarchical features and capture spatial texture variations at multiple scales, enabling highly discriminative classification of surface defects. The results clearly indicate that deep learning-based feature representation through convolutional layers significantly enhances detection accuracy compared to conventional machine learning approaches, establishing the CNN as the most reliable and robust model for automated surface defect classification in industrial applications.

5. CONCLUSION

The research demonstrates the effectiveness of the proposed Deep Depthwise Separable Convolutions for High-Resolution Line-Scan Inspection. Using Xception-based deep feature extraction combined with traditional machine learning classifiers and a proposed CNN model, the system achieves robust and accurate defect classification across six defect classes: Crazing, Inclusion, Patches, Pitted, Rolled, and Scratches. Among the existing methods, the Passive Aggressive Classifier performs better than SGD and QDA, achieving 96.39% accuracy and a macro-average AUC of 97.89%, while the SGD classifier achieves 94.28% accuracy with an AUC of 96.44%. The QDA classifier shows comparatively lower performance with 84.34% accuracy and 90.47% AUC, mainly due to higher inter-class overlap. In contrast, the Proposed CNN model significantly outperforms all existing approaches, achieving an overall accuracy of 98.19%, precision of 98.13%, recall of 98.17%, and F1-score of 98.11%, confirming its superior learning and generalization capability. Further analysis using class-wise metrics, confusion matrices, and ROC curves validates the robustness of the proposed approach. The Proposed CNN achieves 100% recall for critical defect classes such as Inclusion, Patches, Pitted, and Scratches, while maintaining 98% macro-average precision, recall, and F1-score across all classes. The macro-average AUC of 98.91% highlights excellent class separability and reliable multi-class discrimination. Real-time prediction results further confirm the practical

International Journal of
AI Electronics and Nexus Energy
Peer Reviewed, Referred & Indexed Journal
ISSN: 3070-0515 www.zesterapublications.com Original Research Paper

applicability of the system, as the trained model accurately classifies unseen test images with minimal misclassification. Overall, the proposed framework proves to be a highly effective, scalable, and industry-ready solution for automated surface defect inspection in manufacturing environments.

REFERENCES

[1]. Liao, Ruiying, Linghui Yang, Luyao Ma, and Jigui Zhu. "In-motion continuous point cloud measurement based on bundle adjustment fused with motion information of triple scan images." *Optics Express* 30, no.12(2022):21544-21567

[2]. Sundara pandi, Manickam, Sivakumar Shanmugam, and Ramasamy Ramaraj. "Tuning Cu2O shell on gold nano cube core employing amine-functionalized silane for electrocatalytic nitrite detection." *ACS Applied Nano Materials* 5, no. 1 (2022): 1674-1682.

[3]. Zabulis, Lukas, Arunas Lipnickas, and Rytis Augustauskas. "Application of computer vision methods for automated wooden planks length measurement." In *2022 18th Biennial Baltic Electronics Conference (BEC)*, pp. 1-6. IEEE, 2022.

[4]. Seong, Daewoon, Deokmin Jeon, Ruchire Eranga Wijesinghe, Kibeom Park, Hyeree Kim, Euimin Lee, Mansik Jeon, and Jeehyun Kim. "Space-time division multiplexing-based superfast spectral-domain optical coherence tomography up to 1 MHz A-scan rate." In *Frontiers in Ultrafast Optics: Biomedical, Scientific, and Industrial Applications XXII*, vol. 11991, pp. 67-72. SPIE, 2022.

[5]. Le, Nhan, Jie Lu, Peijun Tang, Kwok-Hung Chung, Hrebesh Subhash, LaTonya Kilpatrick-Liverman, and Ruikang K. Wang. "Intraoral optical coherence tomography and angiography combined with autofluorescence for dental assessment." *Biomedical Optics Express* 13, no. 6 (2022): 3629-3646.

[6]. Zhu, Bin, Yiqiang Wang, Jiří Dluhoš, Andy J. London, Michael Gorley, Mark J. Whiting, and Tan Sui. "A novel pathway for multiscale high-resolution time-resolved residual stress evaluation of laser-welded Eurofer97." *Science advances* 8, no. 7 (2022): eabl4592.

[7]. Ginner, Laurin, Simon Breuss, and Lukas Traxler. "Fast inline microscopic computational imaging." *Sensors* 22, no. 18 (2022): 7038.

[8]. Jiang, Xiaoyun, Teng Liu, Vimal Prabhu Pandiyan, Emily Slezak, and Ramkumar Sabesan. "Coarse-scale opt retinography (CoORG) with extended field-of-view for normative characterization." *Biomedical Optics Express* 13, no. 11 (2022): 5989-6002.

[9]. Albanese, A. Nardello, M., Fiacco, G. and Brunelli, D., 2022. Tiny machine learning for high accuracy product quality inspection. *IEEE Sensors Journal*, *23*(2), pp.1575-1583.

[10]. Huang, Peng, Chenghao Liu, Xiaoying Yang, Dongwang Yi, and Han Zhang. "High-speed measurement system for cord-rubber composites on conveyor belt based on machine vision." In *5th International Conference on Informatics Engineering and Information Science (ICIEIS 2022)*, vol. 12452, pp. 62-68. SPIE, 2022.

[11]. Zeng, Yingjun, Guochun Chen, Fuxin Zhao, Chao Wu, Lida Xu, Yansong Zhang, Wenjie Wu et al. "Metal-based sandwich type thick-film platinum resistance temperature detector for in-situ temperature monitoring of hot-end components." *Applied Surface Science* 637 (2023): 157979.

[12]. Breyton, Grégoire, Hakim Amara, Jaysen Nelayah, Jérôme Creuze, Hazar Guesmi, Damien Alloyeau, Guillaume Wang, and Christian Ricolleau. "Atomic-scale surface segregation in Copper-Gold nanoparticles." *Physical Review Letters* 130, no. 23 (2023): 236201.

International Journal of
AI Electronics and Nexus Energy
Peer Reviewed, Referred & Indexed Journal
ISSN: 3070-0515 www.zesterapublications.com Original Research Paper

[13]. Dawson, Karl, Fabian Duarte-Martinez, Simon Gray, John Nicholls, G. Gibson, J. Leggett, and G. J. Tatlock. "Environmentally assisted cracking of a single crystal nickel-based superalloy." *Materials at High Temperatures* 40, no. 4 (2023): 296-307.

[14]. Chen, Kai, Adrianna Mackiewicz, Hans-Peter Seifert, Sannakaisa Virtanen, and Stefan Ritter. "Role of Zn injection on mitigating stress corrosion cracking initiation of Alloy 182 weld metal in simulated light water reactor environment." *Corrosion Science* 221 (2023): 111364.

[15]. Illing, Cyprian, Zhe Ren, and Frank Ernst. "Low-Temperature Carburization: Ex Situ Activation of Austenitic Stainless Steel." *Metals* 13, no. 2 (2023): 335.

[16]. Tang, Bo, Li Chen, Wei Sun, and Zhong-kang Lin. "Review of surface defect detection of steel products based on machine vision." *IET Image Processing* 17, no. 2 (2023): 303-322.